ELSEVIER

Surface Science 330 (1995) 182–192

surface science

Structural analysis of the two c(2 × 2) phases of Na adsorbed on Al(100)

W. Berndt *, D. Weick, C. Stampfl, A.M. Bradshaw, M. Scheffler

Fritz-Haber-Institut der Max-Planck-Gesellschaft, Faradayweg 4-6, 14195 Berlin, Germany

Received 4 November 1994; accepted for publication 15 February 1995

Abstract

We have studied the adsorption of Na on Al(100) at different substrate temperatures using low-energy electron diffraction (LEED) and density-functional theory (DFT) calculations. Below 180 K and above 260 K well-ordered c(2 × 2) overlayers develop which are completely different in structure. As determined by the LEED intensity analysis the Na atoms in the phase formed at low temperature occupy fourfold hollow sites where the nearest-neighbour Na–Al bond length is 3.27 ± 0.01 Å. The Na atoms in the phase formed above 260 K occupy substitutional sites. For this structure the LEED intensity analysis shows a contraction of the topmost Al interlayer spacing of 9.1% ± 0.5% and a nearest-neighbour Na–Al bond length of 3.07 ± 0.01 Å. On heating, the low-temperature c(2 × 2) structure is irreversibly transformed into the room-temperature structure. The adsorption sites and accompanying substrate relaxations and/or reconstructions agree very closely with those predicted from DFT calculations.

Keywords: Alkali metals; Aluminum; Chemisorption; Density functional calculations; Electron–solid interactions, scattering, diffraction; Low energy electron diffraction (LEED); Low index single crystal surfaces; Surface relaxation and reconstruction

1. Introduction

It has become apparent through recent experimental and theoretical studies that there are strong deviations to the traditional picture of alkali-metal adsorbates on metal surfaces, a picture which originates from the work of Gurney [1]. The long history of alkali-metal adsorption studies is related to the technological importance of these systems in that they induce a lowering of the substrate work function and change the chemical properties of surfaces in catalysis [2,3]. In addition, they have long been regarded as model systems useful for studying the basic mechanism of chemisorption because of their simple electronic structure and the understanding that the adsorption is not complicated by extensive reconstruction. Contrary to this conception that the alkali-metal atoms remain on the surface and occupy the maximally coordinated hollow sites have been reports of unusual adsorption geometries on close-packed metal surfaces. On the more open surfaces, for example {110}, it is well known that surface reconstruction is often induced by alkali-metal adsorption [4,5]. For the $(\sqrt{3} \times \sqrt{3})$R30° structures of Na, K and Rb on Al(111) formed at room temperature, however, it has recently been found that the alkali-metal atoms occupy substitutional sites, i.e. they remove surface Al

* Corresponding author.

SSDI 0039-6028(95)00229-4

atoms and adsorb in their places [6–10]. Studies of Cs on Al(111) also indicate a reconstruction of the surface although no definitive determination of the atomic geometry has as yet been reported [11]. For the K and Rb surface structures on Al(111), the adsorbate geometries are different when created at low temperature and at room temperature, even though both display the same $(\sqrt{3} \times \sqrt{3})$R30° low-energy electron diffraction (LEED) pattern. In the low-temperature structure the adatoms occupy on-top sites, but on warming to room temperature, an irreversible transformation into the substitutional geometry takes place. On-top site adsorption of alkali-metal adatoms, also contrary to expectation, has also been reported for the systems Cs/Cu(111) [12], Cs/Ru(0001) [13], K/Ni(111) [14–17] and K/Cu(111) [16]. Moreover, it has not just been the unexpected adsorbate geometries that have attracted attention recently: There is also an active and ongoing interest in understanding the alkali-metal adsorbate–substrate bond in the low coverage regime [18].

In the present paper we describe a study of the adsorption of Na on the (100) surface of Al by detailed LEED intensity analysis, concentrating in particular on the $c(2 \times 2)$ structure. This adsorption system was investigated some years ago by two independent LEED intensity analyses [19,20] in which it was concluded that Na occupies the hollow site. In both studies the system was annealed to 360 K. However, it has been shown recently using high-resolution core level spectroscopy (HRCLS) [21] and surface extended X-ray absorption fine structure (SEXAFS) measurements [22] that the $c(2 \times 2)$ surface structures are different (although the coverages are the same) when formed at low temperature and at room temperature, and that the structural phase transition is irreversible, just as for the $(\sqrt{3} \times \sqrt{3})$R30° structures of K and Rb on Al(111). The SEXAFS study identified the hollow site as the adsorption site at low temperature; for the room-temperature phase three models for this phase were discussed. Subsequently, from density-functional theory (DFT) calculations [23], it has been predicted that the structure formed at low temperature consists of Na atoms in hollow sites, in agreement with experiment, and that the structure formed at room temperature corresponds to substitutional Na adsorption.

2. Experimental

2.1. Apparatus

The experiments were carried out in a conventional ultra-high vacuum (UHV) apparatus equipped with a three-grid LEED/Auger system. Auger electron spectroscopy (AES) was performed using the LEED optics in the retarding-field mode in combination with an auxiliary glancing-incidence electron gun. A quadrupole mass spectrometer was applied to analyse the residual gas in the vacuum chamber (base pressure of about 2×10^{-10} mbar) as well as to check the purity of the argon gas used for surface cleaning treatments by ion sputtering. The Al crystal of dimensions 8 mm × 6 mm × 3 mm was cut from bulk material by spark erosion. Its surface, mechanically and electrochemically polished using standard methods, was oriented to within 0.5° of the ⟨100⟩ direction. The specimen was mounted on a U-shaped tungsten wire with which it could be heated electrically and/or cooled by liquid nitrogen down to about 90 K. For temperature measurements a thin NiCr/Ni thermocouple was fixed in a hole at the edge of the crystal. Temperature changes of defined rates could be applied by means of a programmable control unit. The heating current in the range up to about 20 A was periodically interrupted for a short time during which the temperature-dependent LEED beam intensity was registered free from magnetic field distortion.

2.2. Surface cleaning treatments

In order to clean the (100) surface several cycles of ion bombardment and annealing were needed. During the sputter process an argon pressure of about 2×10^{-4} mbar was maintained in the chamber in order to minimize the re-contamination of the Al surface by chemically reactive ions of the residual gas or of molecules desorbed from the ion gun filament. After each bombardment (500 eV ion beam energy for one hour at a crystal temperature of 600 K) and subsequent annealing at about 580 K for two minutes AES measurements were taken to check the cleanliness of the sample. The most persistent Auger peak appeared at about 53 eV indicating the existence of aluminum oxide [24]. Although Hutchins et

al. [19] and Quinto and Robertson [24] judged the Al surface to be clean for a 1:25 ratio between the Auger amplitudes of the oxide at 53 eV and the metal at 67 eV, we have continued the cleaning process until the ratio reached a limiting value of about 1:180 (Fig. 1).

2.3. Preparation of the Na adsorbate layers

Immediately after cleaning the (100) surface, Na was deposited from a SAES getter source [25] with the crystal held at different temperatures. During evaporation the background pressure increased to about 2×10^{-9} mbar. The layer growth was controlled step by step with LEED. Depending on substrate temperature and coverage a series of different diffraction patterns could be observed. Na atoms adsorbed around room temperature show LEED patterns which, in the sequence of increasing coverage, result from a somewhat disordered c(2 × 2) overlayer containing phase and antiphase domains, a well-ordered c(2 × 2) adlayer and finally a mixture of c(2 × 2) and $(\sqrt{17} \times \sqrt{17})$R14° overlayers. In the case of evaporation at substrate temperatures around 100 K, a disordered $(2\sqrt{2} \times \sqrt{2})$R45° adlayer initially develops which is transformed consecutively into overlayers with the periodicity c(2 × 2), c($7\sqrt{2} \times \sqrt{2}$)R45°, c(8 × 2), 3 × 2 and 7 × 7. The present work focuses on the temperature-dependent c(2 × 2) structures, particularly on their local geometries.

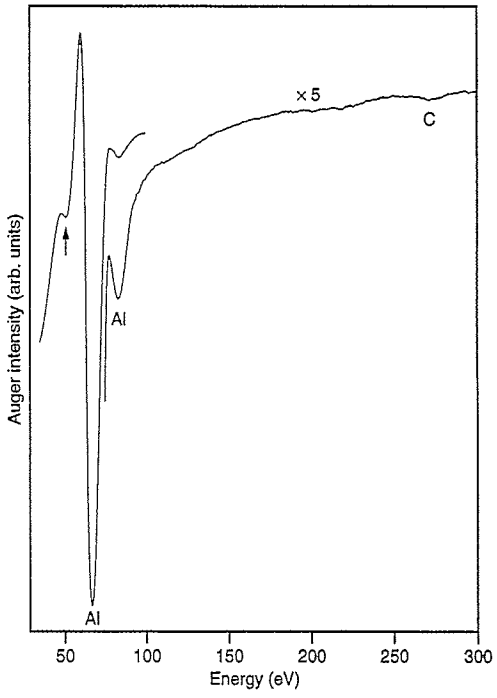

Fig. 1. Auger electron spectrum of the clean Al(100) surface. The arrow indicates the peak assigned to aluminium oxide.

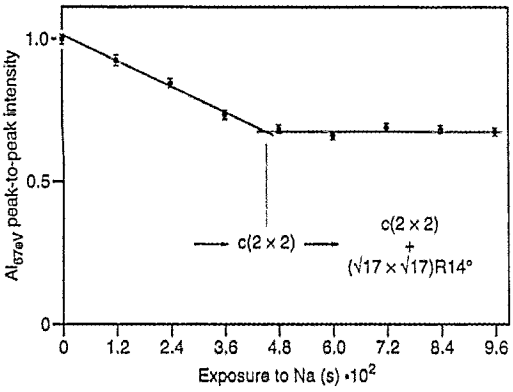

Fig. 2. Normalized peak-to-peak intensity of the Al Auger transition at 67 eV as a function of exposure to Na for crystal temperatures around 300 K.

The deposition of Na atoms at room temperature was additionally monitored by AES. Observation of the Na KLL peaks at the relatively high transition energies around 950 eV was not possible because of electrical isolation problems. Thus the intensity of the Al Auger peak at 67 eV was recorded. Up to the completion of the well-ordered c(2 × 2) structure a linear decrease of the Auger signal height was found indicating monolayer growth of the adsorbate layer (Fig. 2).

2.4. Crystal manipulating facilities

The crystal could be displaced parallel and perpendicular to the direction of the incident LEED beam and rotated about an axis in the surface plane aligned along the ⟨110⟩ direction of the crystal by an angle of $\Theta \approx \pm 60°$, where Θ is the polar angle of incidence. The azimuthal alignment was carefully performed outside the vacuum chamber by use of the Laue diffraction pattern. LEED intensity measurements of symmetry-equivalent LEED beams for off-normal electron incidence then showed an experimental error not greater than that for normal incidence. Θ could be set to within $\pm 0.2°$.

2.5. Diffraction beam intensity measurements

The intensity of the LEED spots on the screen was measured by means of a computer-controlled mirror/photometer system which has been described elsewhere [26]. Intensity-versus-energy ($I(E)$) curves were taken from the clean Al(100) surface (8 curves of symmetry-inequivalent beams at $\Theta = 0°$, 7° and 12°) and from both the c(2 × 2) overlayer phases formed at low temperature and room temperature (15 and 13 curves, respectively, of symmetry-inequivalent beams at $\Theta = 0°$ and 7°) in steps of 1 eV up to about 300 eV beam energy. The time during which a freshly prepared c(2 × 2) adlayer could be studied was limited to about 3 h. Afterwards a gradual increase of background intensity caused the spot intensity to drop by more than the amount of the experimental error without, however, changing the structure of the $I(E)$ curves. Intensity measurements on repeatedly produced c(2 × 2) layers showed an excellent reproducibility of the curves.

3. Theoretical

3.1. LEED intensity calculations

The LEED intensity calculations were carried out using a fully dynamical calculation scheme [27] which includes the possibility of automatic, simultaneous refinement of the structural parameters, the real part of the complex self-energy and the effective Debye temperatures [28]. In the program the "layer KKR (Korringa–Kohn–Rostocker)" approach is used together with the "layer doubling method" [29]. The extent of agreement between experimental and theoretical intensity data was quantified by the reliability factors (r-factors) introduced by Kleinle et al. [30], R_{DE} (discrete energy). The r-factors of Pendry [31], R_p, and Zanazzi and Jona [32], R_{ZJ}, were also used to judge the level of agreement between theory and experiment. The scattering from Al and Na atoms was described using nine phase shifts calculated from the muffin-tin band-structure potentials of Moruzzi et al. [33]. The real part V_{or} of the inner potential was taken to be independent of energy whereas the imaginary part V_{oi} was assumed to be energy dependent according to the equation $V_{oi}(E) = V_{oic}[(E - V_{or})/\mathrm{eV}]^{1/3}$. The constant factor V_{oic} is optimized. Thermally induced vibrations of the atoms were taken into account within the framework of the Debye–Waller approximation, where the effective Debye temperatures of Na and the first three Al layers were refined in the analysis.

3.2. Total-energy density-functional theory calculations

The total-energy density-functional theory calculations were performed using the fhi93cp computer code [34] which uses a plane wave basis set and fully separable, norm-conserving, ab initio pseudopotentials [35]. The energy cut-off was taken to be eight Rydbergs and ten special k-points [36] in the irreducible part of the Brillouin zone were used to replace the $k_{\|}$ summation. A nine-layer Al slab with a vacuum region equivalent to seven such layers was used to model the surface [37] where Na was adsorbed only on the side. The positions of the Na atoms and the first two (or when forces indicated that it may be important, three) substrate layers were relaxed and in the cases where there are Al atoms above the Na atoms, the positions of these Al atoms were also relaxed.

Practically all reasonably possible geometries with a c(2 × 2) surface periodicity were considered. Sites tested were the "on-surface" sites on-top, hollow and bridge. Also the substitutional site was considered, as well as many geometries where there is an Al layer above the Na layer. For further details about the method of calculation we refer to Refs. [10,23].

4. Results and discussion

4.1. The clean Al(100) surface

Before starting the LEED intensity analysis of the Na overlayers on Al(100) we have studied the clean surface. In Fig. 3, a comparison of the experimental and theoretical $I(E)$ curves is presented. The calculated best-fit $I(E)$ curves were obtained for an expansion of the topmost (first) interlayer spacing of about 2.6% ± 0.2% and a slight contraction of the third interlayer spacing of about 0.5% ± 0.4%, which showed values of the reliability factors R_{DE}, R_P and

Table 1
Structural parameters, inner potentials V_{or} and V_{oic}, Debye temperatures Θ_D and r-factors (averaged values) for the low-temperature c(2×2) phase "LT-phase" and the room-temperature c(2×2) phase "RT-phase" obtained from the LEED intensity analysis

	c(2×2)											
	d_{ad} (Å)	d_{12}	d_{23}	Δd_3 (Å)	V_{or} (eV)	V_{oic} (eV)	Θ_D^{Na} (K)	$\Theta_D^{Al,1\_layer}$ (K)	$\Theta_D^{Al,2\_layer}$ (K)	$\langle R_{DE} \rangle$	$\langle R_P \rangle$	$\langle R_{ZJ} \rangle$
"LT-phase"	2.565±0.010	2.032±0.010	2.022±0.010		−4.00±0.30	0.80±0.10	150±25	300±50	350±50	0.322	0.293	0.218
"RT-phase"	1.100±0.030	1.840±0.010	2.040±0.010	0.050±0.020	−5.25±0.30	0.90±0.10	110±10	190±20	290±30	0.233	0.220	0.162

d_{ad} is the vertical distance between the adsorbate and the topmost Al layer, d_{12} and d_{23} are the first and second Al interlayer spacings, respectively. Δd_3 represents the magnitude of rumpling in the third Al layer. The error values correspond to an increase of a geometric average of the three r-factors (Kleinle et al., Pendry, Zanazzi and Jona) by about 1% with respect to a variation of the parameters considered.

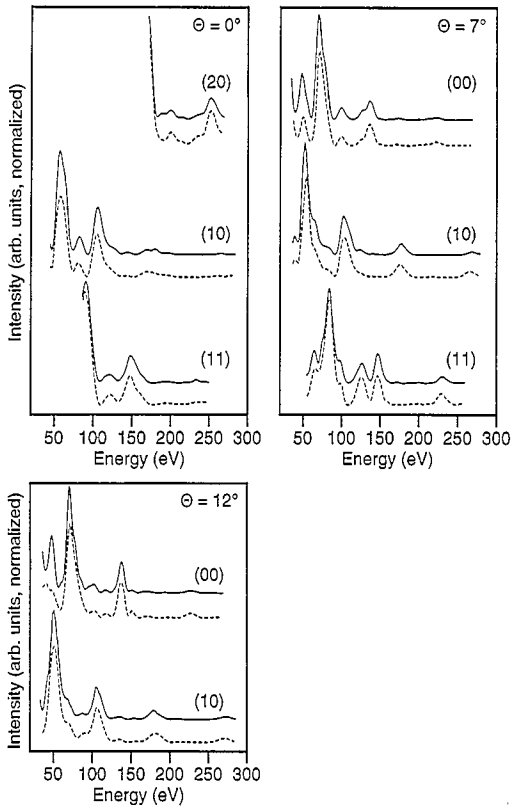

Fig. 3. $I(E)$ curves of the clean Al(100) surface for $\Theta = 0°$, 7° and 12°. (Full line: experiment; broken line: best-fit theory.)

R_{ZJ} of 0.160, 0.182 and 0.112, respectively, averaged over 8 beams. The same trend of relaxation has been reported for Al(111) and Al(100) surfaces in earlier publications [38,39]. Values for V_{or} and V_{oic} of -5.3 ± 0.3 eV and 0.8 ± 0.1 eV, respectively, were found to give best agreement with experiment and the effective Debye temperature for Al in the first, second and third layer was determined to be 280 ± 15 K, 380 ± 20 K and 550 ± 50 K, respectively. For the way the errors were obtained see caption of Table 1.

4.2. The c(2 × 2) adsorbate phases

The $I(E)$ curves obtained from the two c(2 × 2) phases are quite different as demonstrated in Fig. 4. Also shown is the comparison with the corresponding theoretical best-fit curves for (a) the low-temperature and (b) the room-temperature structures. The LEED analysis shows that Na atoms adsorbed at low crystal temperatures occupy fourfold hollow sites on an essentially unrelaxed surface. The Na–Al nearest-neighbour and second-nearest-neighbour bond lengths are determined to be 3.27 and 4.60 Å, respectively. Fig. 5a shows the proposed model of this structure. It agrees very well with the results of the SEXAFS study [22] where a nearest-neighbour Na–Al bond length of 3.21 Å was obtained.

In order to analyse the structure of the room-temperature c(2 × 2) phase we have considered a number of models involving unreconstructed and reconstructed surfaces with the Na atoms in simple as well as in substitutional adsorption sites. In this case our results do not confirm any of the models (favoured or not) proposed in the SEXAFS study mentioned above. The only model tested which leads to a satisfactory agreement with experiment is illustrated in Fig. 5b: Every second Al surface atom is substituted by a Na atom jutting out of the surface plane

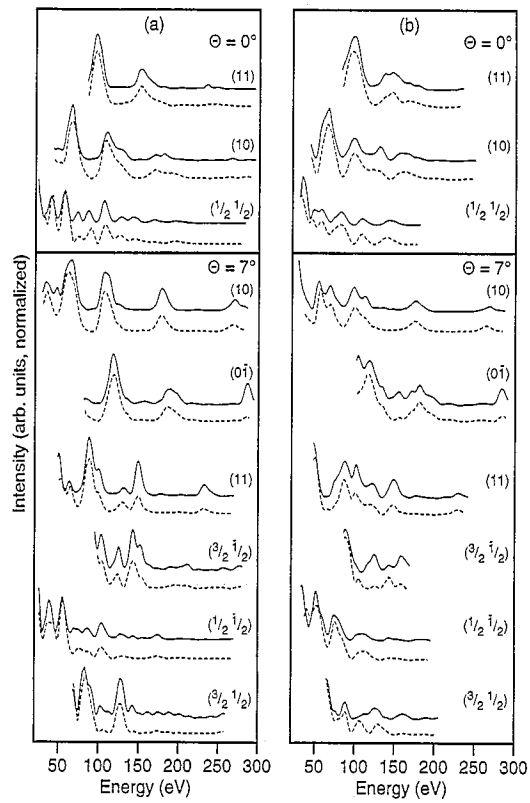

Fig. 4. $I(E)$ curves of the low-temperature c(2×2) phase (a) and the room-temperature c(2×2) phase (b) for $\Theta = 0°$ and 7°. (Full line: experiment; broken line: best-fit theory.)

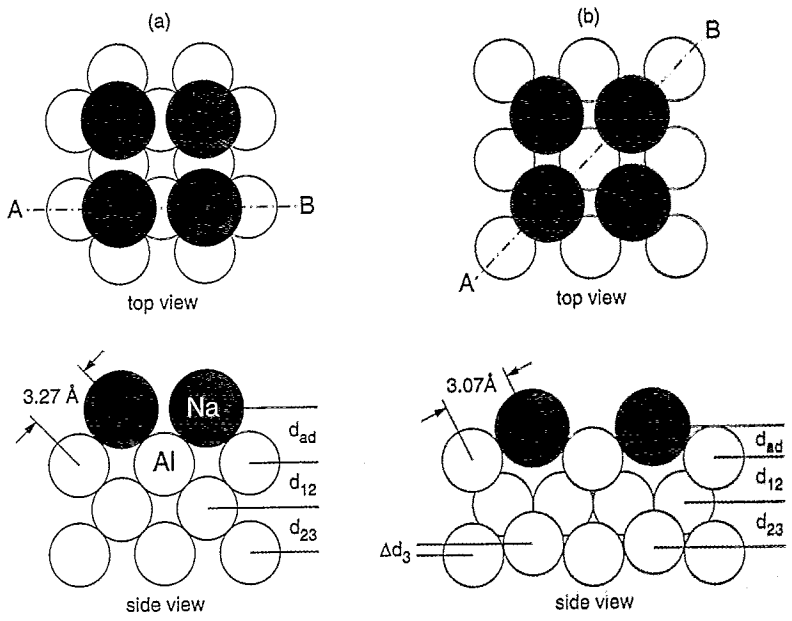

Fig. 5. Hollow-site model for the low-temperature structure (a) and substitutional model for the room-temperature structure (b) (top views and side views along the directions A–B). d_{ad} is the vertical distance of the adsorbate from the topmost Al layer; d_{12} and d_{23} are the first and second Al interlayer spacings, respectively, and Δd_3 is the rumpling of the Al atoms in the third layer.

by 1.10 Å because of its larger effective radius. Consequently, the Na–Al nearest-neighbour and second-nearest-neighbour bond lengths are 3.07 and 3.57 Å, respectively. Between the topmost (first) and the second Al layer a distance of $d_{12} = 1.84$ Å is found which corresponds to a contraction of 9.1% with respect to the bulk interlayer spacing of 2.025 Å. In Table 1 the structural and non-structural parameters of the LEED intensity analysis are given along with the corresponding r-factors (averaged values) for both c(2 × 2) structures.

The search for reasonable structure models for the room-temperature phase was greatly simplified by DFT calculations [23] which predicted a substitutional adsorption geometry for the Na atoms as the stable structure. Table 2 represents a list of calculated adsorption energies and structural parameters for some different adsorption geometries. Models

Table 2
Adsorption energies E_{ad} and structural parameters obtained from total-energy DFT calculations

Site	E_{ad} (eV)	d_{ad} (Å)	d_{12} (Å)	d_{23} (Å)	d_{34} (Å)	Δd_1 (Å)	Δd_3 (Å)	d_{nn} (Å)	d_{nnn} (Å)
On-top	1.33	2.46	1.83	1.99		0.31		2.77	3.74
Bridge	1.45	2.64	1.99					2.99	4.84
Hollow	1.59	2.35	1.95	1.97	1.98			3.08	4.30
Substitutional	1.70	1.10	1.81	1.99	1.97		0.05	3.02	3.52

d_{ad} is the vertical distance of the adsorbate from the top-most Al layer. d_{12}, d_{23} and d_{34} denote the first, second and third Al interlayer spacings, respectively. In the case where a rumpled Al layer is involved, the interlayer spacings are given with respect to the Al atoms in the rumpled layer which give the smallest interlayer spacing. Δd_1 and Δd_3 represent the magnitude of the rumpling in the first (topmost) and third Al layer for the on-top and substitutional sites, respectively. Note that for the on-top geometry (which is of course not observed in practice) the Al atoms underneath the Na atoms are shifted in towards the bulk. For the hollow geometry the surface is relaxed only slightly compared to the bulk values. For the substitutional site the Al atoms in the third layer with lateral positions the same as the Na atoms are displaced upwards towards the surface by 0.03 Å and the alternative Al atoms are displaced in towards the bulk by 0.02 Å, relative to the median positions, d_{nn} and d_{nnn} are the nearest-neighbour and second-nearest-neighbour Na–Al distances, respectively. The theoretical bulk Al lattice constant is 3.98 Å (4.05 Å for the experimental value) corresponding to an ideal interlayer spacing of 1.99 Å for the (100) surface.

were also considered with Al atoms located above the Na layer, such as, for example, the models discussed in the SEXAFS study for the room-temperature c(2 × 2) structure [22]. All of these models, however, were found to be more than 1 eV less favourable than the normal "on-surface" structures. From the adsorption energy point of view the substitutional configuration is preferred and, as shown above, the most favourable one in our LEED intensity analysis. Moreover, we note that both the DFT and LEED methods lead to comparable interatomic distances for the hollow and substitutional geometry, respectively, as can be seen from Tables 1 and 2. The hollow site has the next most favourable adsorption energy. An additional geometry was considered with two Na atoms in a unit cell with twice the area of that of the c(2 × 2) cell, namely $(2\sqrt{2} \times \sqrt{2})$R45°, one in the hollow site and one in the substitutional site. We find the value of the adsorption energy for this mixed hollow-substitutional structure is between that of the hollow and substitutional sites. The result that the Na atoms at low substrate temperatures are adsorbed in energetically less favourable on-surface hollow sites can be understood by assuming that an activation energy is required for the structural rearrangement.

We have tried to refine the structure model for the room-temperature phase by assuming a rumpling of the Al atoms in the third substrate layer because they are positioned at different distances from the next-nearest Na atoms (see Fig. 5b). The LEED analysis shows that the *r*-factors are reduced by about 5% assuming a rumpling of $\Delta d_3 = 0.05$ Å which is also obtained from DFT calculations (see Table 2). In both cases the same tendency is found: Al atoms with lateral positions the same as the Na atoms are displaced upwards towards the surface and the alternative Al atoms are displaced in towards the bulk.

The nearest-neighbour Na–Al distance determined by the LEED analysis is shorter for the substitutional site than for the hollow site, compare 3.07 to 3.27 Å, corresponding to effective Na radii of 1.64 and 1.84 Å, respectively. This result suggests a different bonding nature of Na and Al for the two sites. We note that Na in the more open substitutional site could be regarded as being more highly coordinated than in the hollow site. Both geometries, however, give rise to a similar work function change [40] and therefore surface dipole moment (same coverage). Assuming a simple picture for the adsorbate-induced dipole moment, namely that the dipole moment can be expressed as the product of the adsorbate charge and the distance separating the adsorbate and the center of gravity of the screening charge density, then from the fact that the adsorbate–substrate height d_{ad} for Na in the hollow site is more than twice that for the substitutional site (see Table 1), this indicates a larger transfer of adsorbate charge in the case of substitutional adsorption and correspondingly a larger degree of ionicity and shorter bond length. This is indeed consistent with the fact that the Na–Na interaction is much weaker for the substitutional geometry than for the "normal" on-surface geometry; thus, the dipole depolarization effect is weaker as well. Indication of a similar deviation in the type of bonding for alkali-metal atoms in substitutional sites compared to on-surface sites has been reported for the $(\sqrt{3} \times \sqrt{3})$R30° structures of K and Na on Al(111) [10,41].

On warming, the low-temperature phase yields $I(E)$ curves which are identical to those obtained from the room-temperature phase. Recooling the c(2 × 2) overlayer, however, has no influence on the $I(E)$ curves. We therefore conclude – in agreement with the HRCLS and SEXAFS results [21,22] – that an irreversible transition from the low-temperature to the room-temperature c(2 × 2) structure takes place. We have checked the completeness of the phase transition by subtracting the "low-temperature" $I(E)$ curves from the corresponding "room-temperature" $I(E)$ curves. Since the intensity values for the difference curve have to be positive over the whole energy range, we can estimate that the contribution from Na atoms in "low-temperature" positions must be less than 10%.

The formation of two different overlayer structures at the same coverage and with the same periodicity suggests that it would be interesting to study the way in which the phase transition takes place. Experimental observations of this effect are described and discussed in the following subsection.

4.3. The transition range between the two phases

In order to obtain information on the structural changes in the overlayer associated with the phase

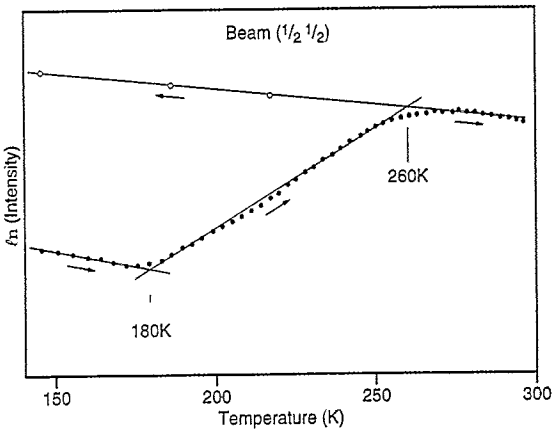

Fig. 6. Intensity of the beam $(\frac{1}{2}\ \frac{1}{2})$ as a function of substrate temperature ($\Theta = 0°$, beam energy = 30 eV). The arrows indicate the direction of the temperature variation.

transition we have taken $I(E)$ curves for the $(\frac{1}{2}\ \frac{1}{2})$ and (1 0) beams as well as a series of LEED patterns as the low-temperature c(2 × 2) phase was warmed very slowly from 90 K to about 400 K. The beginning of the phase transition is clearly indicated by the onset of changes in the form of the $I(E)$ curves of both the $(\frac{1}{2}\ \frac{1}{2})$ and (1 0) beams at about 180 K. After the temperature has reached values around 250 K no further changes occur and the curves are identical to those due to the room-temperature phase. The value of 180 K compares well with the value of 160 K as reported in the HRCLS study [21] and with the value of 180 K estimated from DFT calculations [23].

As an example we show in Fig. 6 the intensity of the adsorbate-induced $(\frac{1}{2}\ \frac{1}{2})$ spot at 30 eV beam energy as a function of temperature for a c(2 × 2) layer of Na prepared at 140 K. With increasing substrate temperature the initial exponential intensity decrease (due to the Debye–Waller effect) obtained for the low-temperature phase changes near 180 K into an increase which continues to about 260 K. At this temperature the transition into the room-temperature phase is complete as indicated by the exponential decrease in the spot intensity which follows. On subsequent cooling, moreover, this latter exponential intensity behaviour extends in the opposite direction (open circles, Fig. 6), thus demonstrating clearly the irreversibility of the transition.

Within the whole transition range the diffraction pattern shown in Fig. 7 is obtained. All LEED spots show weak satellites which are somewhat elongated in the ⟨100⟩ directions and move continuously with increasing temperature towards the nearest integral

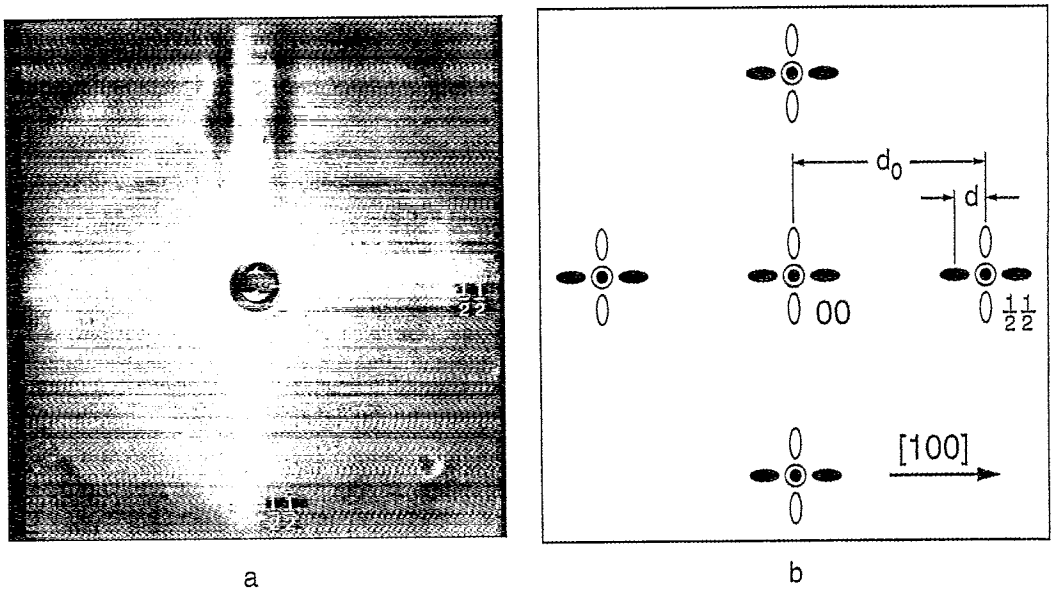

Fig. 7. Photograph (a) and schematic representation (b) of the LEED pattern of the low-temperature c(2 × 2) phase at 200 K for 32.4 eV beam energy. Open and filled spots in (b) designate domains of different orientation. The mean lateral separation between strips of the same local adsorption geometry corresponds to about 6 substrate bulk lattice constants.

or half-order spot positions. A possible explanation for this behaviour is as follows: As the substrate temperature is increased more and more Na adatoms are displaced from their hollow sites to substitutional positions forming c(2 × 2) domains of the room-temperature phase. When the statistical distributions of both the size of the domains and their separations become sufficiently narrow, satellite diffraction features occur. In particular, from the shape of the satellites we conclude that the domains take the form of strips extended perpendicular to the direction of spot elongation. Because of the two directions of elongation the overlayer is assumed to consist of two kinds of domain rotated by 90° with respect to each other. The reciprocal value of the relative distance between the satellites and their nearest integral or half-order spots, $D = d_0/d$, is equal to the mean lateral separation between recurring strips of the same local adsorption geometry. Higher-order satellite spots are suppressed because the separations differ in length (see for example Ref. [42]). With increasing temperature the "room-temperature" strips become broader at the expense of the "low-temperature" strips which leads to an increased mean separation D and, consequently, to an apparent continuously reduced distance d.

On the microscopic level, the phase transition may be considered to proceed in the following way: Na atoms in the fourfold-hollow "low-temperature" positions expel every second Al atom from their surface sites and drop down into the created vacancies. Due to their larger size they jut out of the surface by about 1.1 Å. The dislodged Al atoms are either trapped, for example at steps, or they are located in hollow sites next to "low-temperature" Na atoms which also gives rise to substitutionally adsorbed Na characteristic of the room-temperature phase. The occurrence of these two processes leading to the substitutional geometry ensures that displaced Al atoms are efficiently used up to form a well-ordered reconstructed overlayer.

5. Conclusions

The arrangement of Na atoms in the c(2 × 2) layer on Al(100) strongly depends on the substrate temperature at which the deposition takes place. At low temperatures the Na atoms adsorb in fourfold hollow sites on the unreconstructed surface. Deposition of Na around room temperature (as well as heating of the system prepared at low temperature) results in an adsorbate-induced surface reconstruction after which the adatoms are located in substitutional sites. In order to form the room-temperature phase an activation energy is required. Once adsorbed in the energetically most favourable substitutional sites the Na atoms do not revert to the fourfold hollows when the crystal temperature is lowered. The irreversible phase transition occurs over a temperature range of about 75 K probably as a result of two processes: direct substitution as well as migration of displaced Al atoms to positions between Na atoms in hollow sites.

References

[1] R.W. Gurney, Phys. Rev. 47 (1935) 2798.
[2] H.P. Bonzel, A.M. Bradshaw and G. Ertl, Eds., Physics and Chemistry of Alkali Metal Adsorption (Elsevier, Amsterdam, 1989).
[3] H.P. Bonzel and G. Pirug, in: The Chemical Physics of Solid Surface: Coadsorption, Promotors and Poisons, Eds. D.A. King and D.P. Woodruff (Elsevier, Amsterdam, 1993).
[4] B.E. Hayden, K.C. Prince, P.J. Davie, G. Paolucci and A.M. Bradshaw, Solid State Commun. 48 (1983) 325.
[5] R.J. Behm, in: Physics and Chemistry of Alkali-Metal Adsorption, Eds. H.P. Bonzel, A.M. Bradshaw and G. Ertl (Elsevier, Amsterdam, 1989).
[6] A. Schmalz, S. Aminpirooz, L. Becker, J. Haase, J. Neugebauer, M. Scheffler, D.R. Batchelor, D.L. Adams and E. Bøgh, Phys. Rev. Lett. 67 (1991) 2163.
[7] C. Stampfl, M. Scheffler, H. Over, J. Burchhardt, M.M. Nielsen, D.L. Adams and W. Moritz, Phys. Rev. Lett. 69 (1992) 1532; Phys. Rev. B 49 (1994) 4959.
[8] M.M. Nielsen, J. Burchhardt, D.L. Adams, E. Lundgren and J.N. Andersen, Phys. Rev. Lett. 72 (1994) 3370.
[9] G. Scragg, B.C.C. Cowie, M. Kerkar, D.P. Woodruff, A. Daimellah, S. Turton and R.G. Jones, J. Phys: Condensed Matter 6 (1994) 1869.
[10] J. Neugebauer and M. Scheffler, Phys. Rev. B 46 (1992) 16067.
[11] J.N. Andersen, E. Lundgren, R. Nyholm and M. Qvarford, Surf. Sci. 289 (1993) 307.
[12] S. Lindgren, L. Walldén, J. Rundgren, P. Westrin and J. Neve, Phys. Rev. B 28 (1983) 6707.
[13] H. Over, H. Bludau, M. Skottke-Klein, G. Ertl, W. Moritz and C. Campbell, Phys. Rev. B 45 (1992) 8638.
[14] D. Fisher, S. Chandavarkar, I.R. Collins, R. Diehl, P. Kaukasoina and M. Lindroos, Phys. Rev. Lett. 68 (1992) 2786.

[15] Z. Huang, L.Q. Wang, A.E. Schach von Wittenau, Z. Hussain and D.A. Shirley, Phys. Rev. B 47 (1993) 13626.
[16] D.L. Adler, I.R. Collins, X. Liang, S.J. Murray, G.S. Leatherman, K.-D. Tsuei, E.E. Chaban, S. Chandavarkar, R. McGrath, R.D. Diehl and P.H. Citrin, Phys. Rev. B 48 (1993) 17445.
[17] R. Davis, X.M. Hu, D.P. Woodruff, K.U. Weiss, R. Dippel, K.M. Schindler, Ph. Hofmann, V. Fritzsche and A.M. Bradshaw, Surf. Sci. 307–309 (1994) 632.
[18] J. Bormet, J. Neugebauer and M. Scheffler, Phys. Rev. B 49 (1994) 17242, and references therein.
[19] B. Hutchins, T. Rhodin and J. Demuth, Surf. Sci. 54 (1976) 419.
[20] M. Van Hove, S.Y. Tong and N. Stoner, Surf. Sci. 54 (1976) 258.
[21] J.N. Andersen, E. Lundgren, R. Nyholm and M. Qvarford, Phys. Rev. B 46 (1992) 12784.
[22] S. Aminpirooz, A. Schmalz, N. Pangher, J. Haase, M.M. Nielsen, D.R. Batchelor, E. Bøgh and D.L. Adams, Phys. Rev. B 46 (1992) 15594.
[23] C. Stampfl, J. Neugebauer and M. Scheffler, Surf. Sci. 307–309 (1994) 8; Surf. Rev. Lett. 1 (1994) 222.
[24] D.T. Quinto and W.D. Robertson, Surf. Sci. 27 (1971) 645.
[25] SAES Getters SpA, Milano, Italy.
[26] W. Berndt, Rev. Sci. Instrum. 53 (1982) 221.
[27] W. Moritz, J. Phys. C 17 (1983) 353.
[28] H. Over, U. Ketterl, W. Moritz and G. Ertl, Phys. Rev. B 46 (1992) 15438.
[29] J.B. Pendry, Low Energy Electron Diffraction (Academic Press, London, 1974).
[30] G. Kleinle, W. Moritz and G. Ertl, Surf. Sci. 238 (1990) 119; G. Kleinle, W. Moritz, D.L. Adams and G. Ertl, Surf. Sci. 219 (1989) L 637.
[31] J.B. Pendry, J. Phys. C 13 (1980) 937.
[32] E. Zanazzi and F. Jona, Surf. Sci. 62 (1977) 61.
[33] V. Moruzzi, J. Janak and A. Williams, Calculated Electron Properties of Metals (Pergamon, New York, 1978).
[34] R. Stumpf and M. Scheffler, Computer Phys. Commun. 79 (1994) 447.
[35] X. Gonze, P. Käckell and M. Scheffler, Phys. Rev. B 41 (1990) 12264;
X. Gonze, R. Stumpf and M. Scheffler, Phys. Rev. B 44 (1991) 8505.
[36] S.L. Cunningham, Phys. Rev. B 10 (1974) 4988.
[37] Several of the structures tested were calculated using five Al layers and five special k-points, but due to the unfavourable adsorption energies more detailed calculations were not performed.
[38] F. Jona, D. Sondericker and P.M. Marcus, J. Phys. C 13 (1980) L 155.
[39] H.B. Nielsen and D.L. Adams, J. Phys. C 15 (1982) 615.
[40] J. Paul, J. Vac. Sci. Technol. A 5 (1987) 664.
[41] C. Stampfl, M. Scheffler, H. Over, J. Burchhardt, M. Nielsen, D.L. Adams and W. Moritz, Surf. Sci. 287/288 (1993) 418.
[42] J.E. Houston and R.L. Park, Surf. Sci. 21 (1970) 209.